Electronic Supplementary Material (ESI) for Soft Matter.

Supporting Information

Rapidly Responsive Smart Adhesive-Coated Micropillars Utilizing Catechol-Boronate Complexation Chemistry

*Ameya R. Narkar[1], Chito Kendrick[2], Kishan Bellur[3], Timothy Leftwich[4], Zhongtian Zhang,[1] and Bruce P. Lee[1,]**

[1]Department of Biomedical Engineering, Michigan Technological University, Houghton, MI 49931.

[2]Department of Electrical and Computer Engineering, Michigan Technological University, Houghton, MI 49931.

[3]Department of Mechanical Engineering-Engineering Mechanics, Michigan Technological University, Houghton, MI 49931.

[4]Department of Materials Science and Engineering, Michigan Technological University, Houghton, MI 49931.

Eperimental Section

Protocol for silicon (Si) master mold fabrication

For the fabrication of the Si master, a Si wafer (University Wafer; South Boston, MA) with 100 nm of silicon dioxide (SiO_2) was used as the base substrate. The wafer was solvent cleaned in acetone, isopropanol, and deionized (DI) water before dehydrating at 200°C for 5 min. For the patterning process, a photoresist, Shipley 1813 (Shipley; Marlborough, MA) was spun on at 4000 rpm for 40 sec and baked at 100°C, before exposing in a EV 620 mask alignment system (EV Group; Albany, NY) to give a dose of 160 mW/cm^2. The photomask used had 10 µm diameter pores spaced in a square array with a 20 µm pitch. The developed wafer was hard baked at 120°C for 10 min, and then the SiO_2 was etched in 10:1 buffered oxide etchant (BOE) to produce openings to the Si surface. To etch the Si wafer, a pseudo Bosch etch process was used in a Trion ICP/RIE Etch PHTII-4301 (Trion Technology, Inc.; Clearwater, FL). 100 standard cubic centimeters per minute (sccm) of sulfur hexafluoride (SF_6) was used to etch the Si at a reactor pressure of 35 mTorr, inductively coupled plasma power of 600W, and RIE (Reactive Ion Etch) power of 60 W for 13 sec. 75 sccm of octafluorocyclobutane (C_4F_8) was used to passivate the Si sidewall at a reactor pressure of 120 mTorr, while maintaining inductively coupled plasma power of 600 W for 40 sec. These two steps were cycled 10, 24 and 48 times to achieve around 4, 10 and 20 µm deep pores, respectively. The photoresist and SiO_2 were removed in acetone and BOE, respectively, to complete the Si master fabrication.

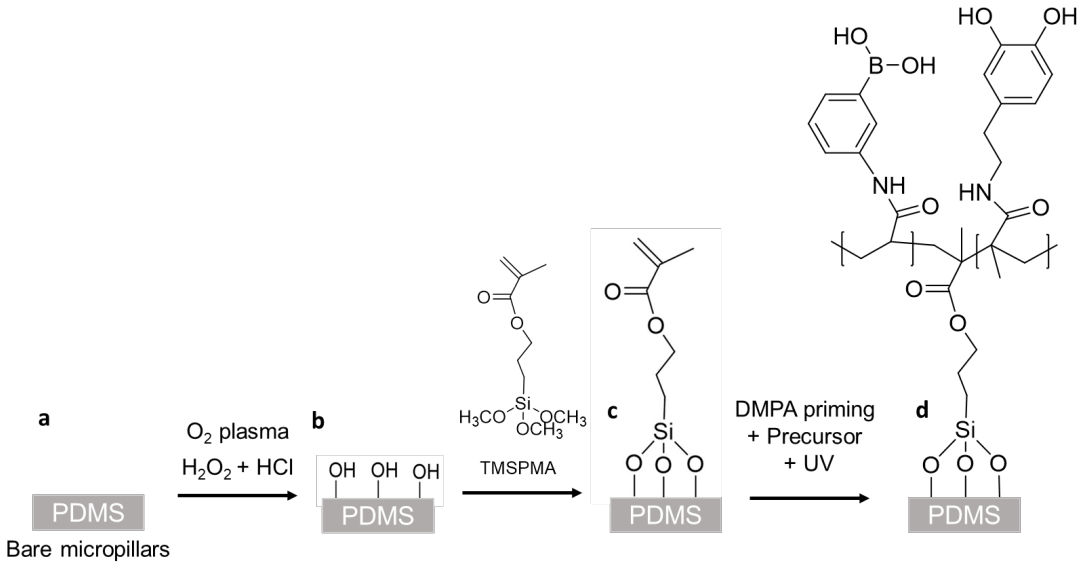

Scheme S1. Schematic representation of a bare micropillars (a) treated with with O_2 plasma and hydrogen peroxide (H_2O_2) with HCl (b), further modified using TMSPMA (c), and after *in situ* UV-initiated polymerization to form the adhesive hydrogel chemically linked to PDMS (d).

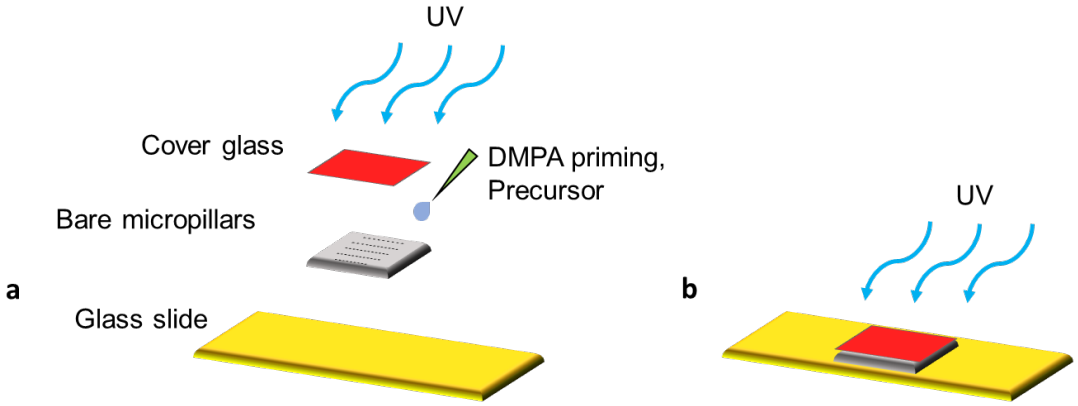

Scheme S2. Schematic representation of the separate components involved in coating the bare micropillars (a) and the assembled configuration (b).

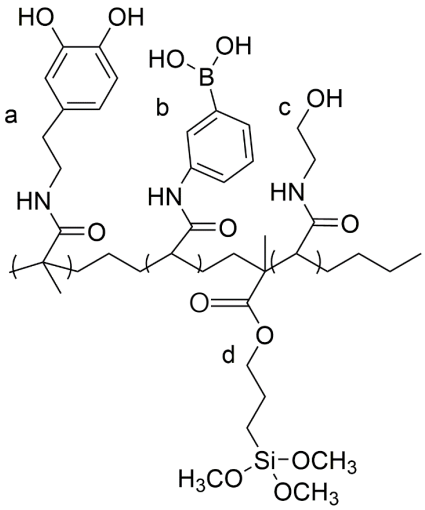

Scheme S3. Chemical structure of the polymer linked to PDMS containing DMA (a), APBA (b), HEAA (c) and TMSPMA (d).

Imaging setup for CA Measurements

The contact angle measurement system comprises of an illumination source, a stage for droplet deposition on the sample and a microscope coupled to CCD camera. A carousel projector (Kodak Medalist, Eastman Kodak Company; Rochester, NY) was used as the source of illumination. A lab jack (L200, Thorlabs; Newton, NJ) was mounted on a translation stage (AXY2509W, Velmex; Bloomfield, NY) enabling X-Y-Z movement of the sample stage. A long-distance microscope (K2/S, Infinity; Boulder, CO) was coupled to a CCD camera (TM-1325CL, Pulnix; Sunnyvale, CA) for focusing and image acquisition. Images were captured on an IBM ThinkPad T60 laptop using the EPIX XCAP software and the EPIX EL1DB frame grabber.

Protocol for XPS analysis

A Mg anode operated at 15 kV, 27 mA and 400 W was used to generate X-rays ($h\upsilon$ = 1253.6 eV) and a hemispherical analyzer angled at 45 degrees from the sample was used to detect electrons from an analysis area with a nominal diameter of 800 μm. Survey spectra were collected for 5 min, in a range of 0 to 1150 electron volts (eV), a step size of 0.8 eV/step, a 20 ms/step dwell time and a 187.85 eV pass energy. High resolution spectra were collected for the time required to generate adequate signal to noise, in a 20 eV range per element (with the combined Cl2p and B1s region spanning a range of 30 eV), a step size of 0.1 eV/step, a 100 ms/step dwell time and a 23.50 eV pass energy. Charge correction was accomplished with a neutralizer that generated 6 eV electrons at a current necessary for the major peak in the C1s region to present at 284.8 eV. For the survey spectra, the number of scans were 10 scans. For the high resolution spectra, the number of scans were 80 scans for B1s,30 scans for N1s, and 5 scans for C1s, Si2p, and O1s.

Results

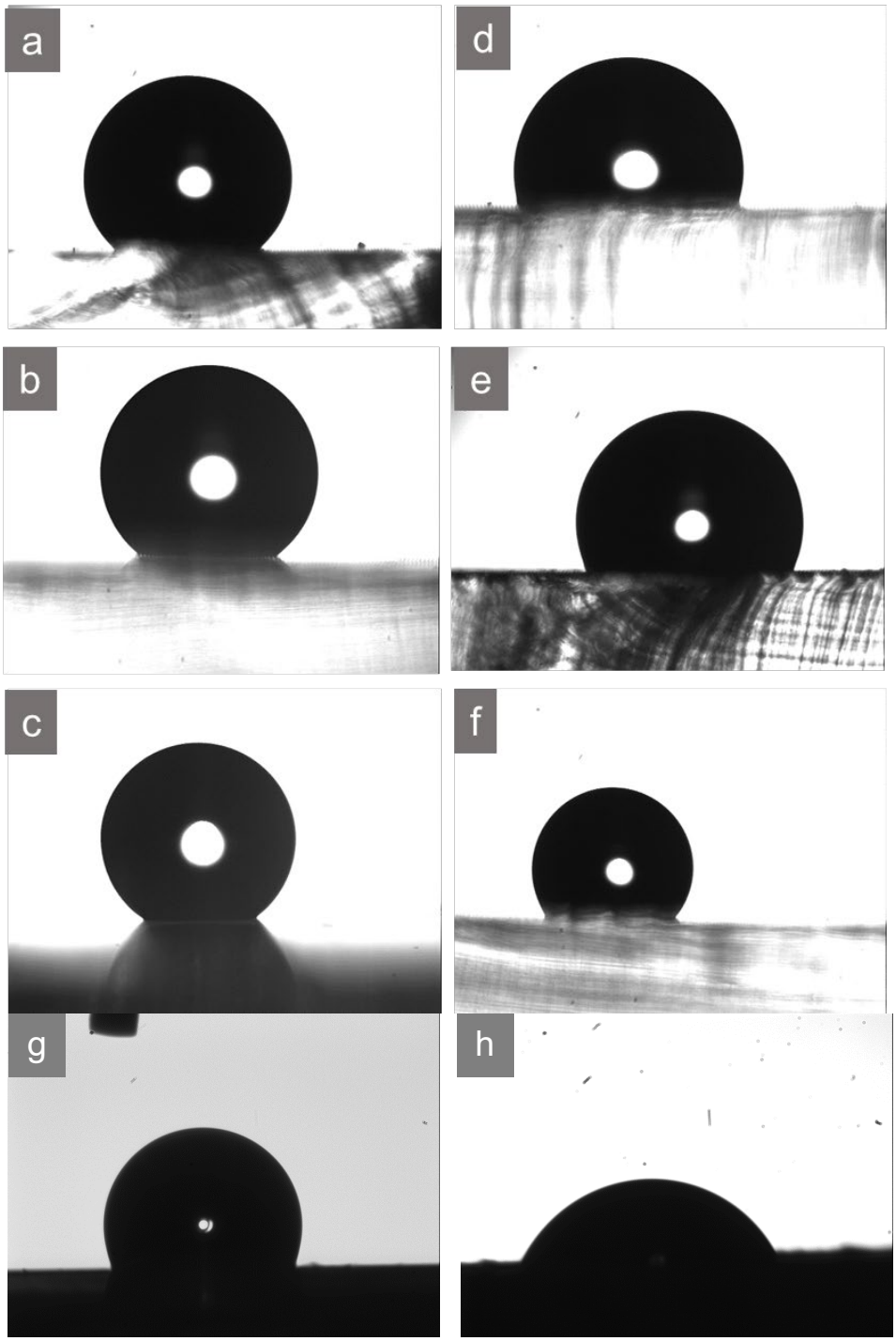

Figure S1. Contact angle images showing representative images of a water drop on the surface of bare (Bare-AR0.4 (a), Bare-AR1 (b), and Bare-AR2 (c)) and adhesive hydrogel-coated (AD-AR0.4 (d), AD-AR1 (e), and AD-AR2 (f)) micropillars as well as flat PDMS (g) and AD-Flat (h).

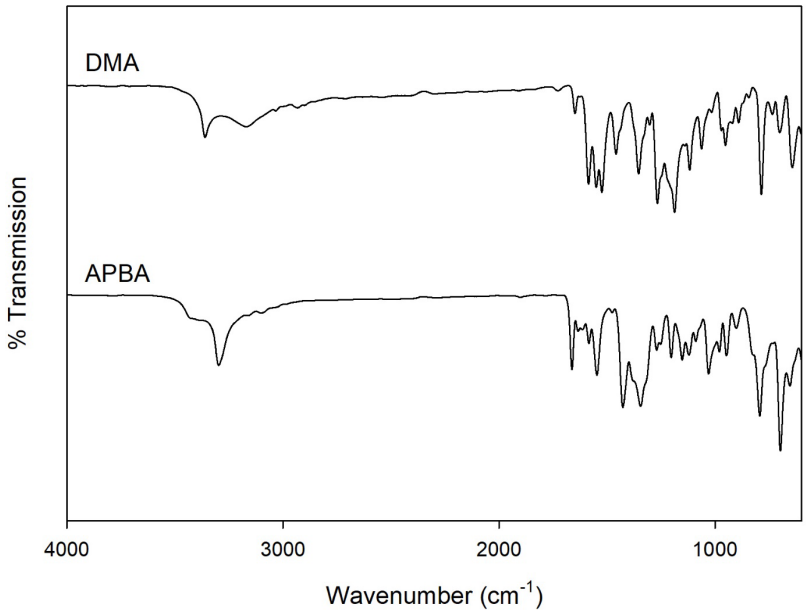

Figure S2. FTIR spectra of DMA and APBA monomers.

Table S1. Statistical analysis for W_{adh} and S_{adh} of AD-Flat, bare templates and adhesive hydrogel-coated structures of different ARs tested at pH 3 (n = 3). W_{adh} or S_{adh} for compositions not connected by the same letter are significantly different.

Composition	W_{adh}	S_{adh}
Bare-AR0.4	A	A
Bare-AR1	A	A
Bare-AR2	A	A
AD-Flat	B	A
AD-AR0.4	B	B
AD-AR1	C	B
AD-AR2	A	A

Table S2. Statistical analysis for W_{adh} and S_{adh} of AD-Flat, bare templates and adhesive hydrogel-coated structures of different ARs tested at pH 9 (n = 3). W_{adh} or S_{adh} for compositions not connected by the same letter are significantly different.

Composition	W_{adh}	S_{adh}
Bare-AR0.4	A	A
Bare-AR1	A	A
Bare-AR2	A	A
AD-Flat	B	A
AD-AR0.4	A	A
AD-AR1	A	A
AD-AR2	A	A

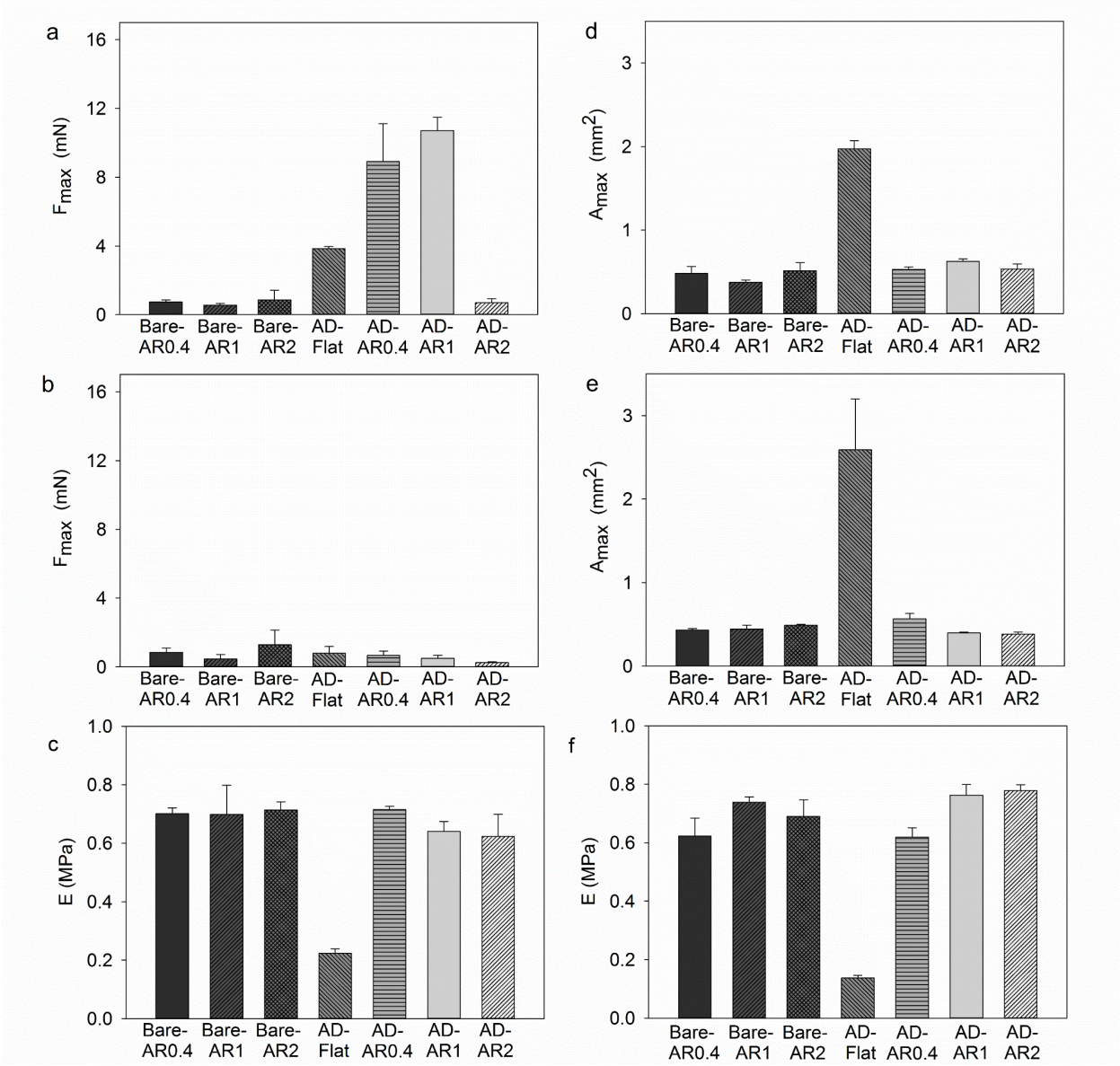

Figure S3. F_{max} (a, b), A_{max} (d, e) and E (c, f) for adhesive tested at pH 3 (a, b, c) and 9 (d, e, f) (n = 3).

Scheme S4. Schematic representation of the smart adhesive depicting pH-dependent catechol-boronate complexation (pH 9) and surface interaction (pH 3).

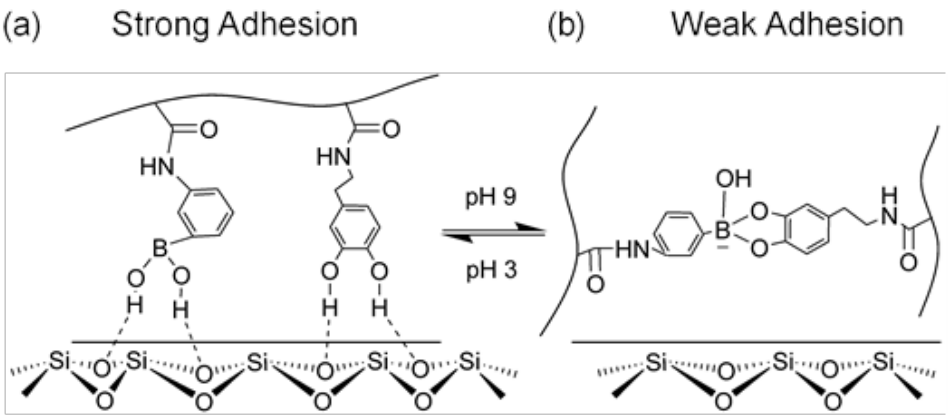

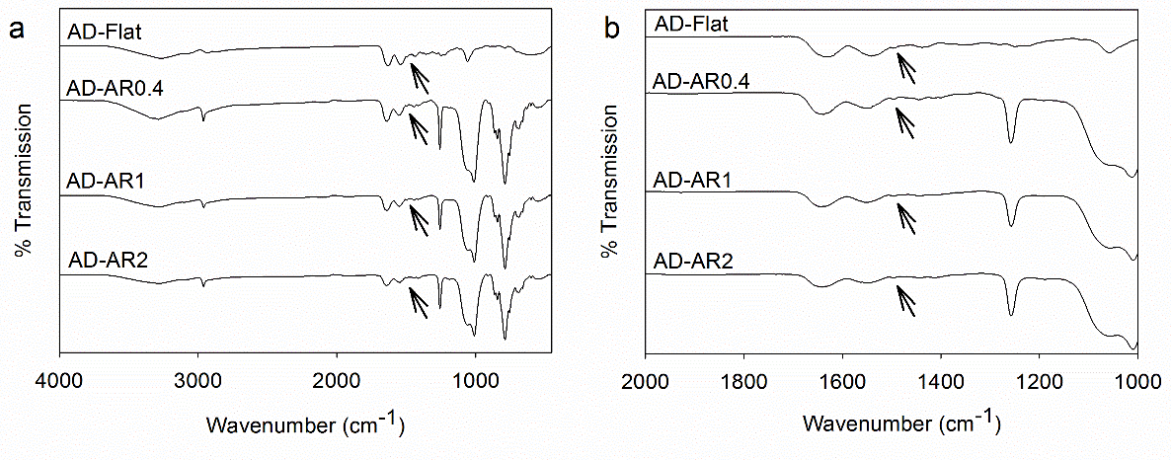

Figure S4. FTIR spectra of AD-Flat, AD-AR0.4, AD-AR1 and AD-AR2 (in the entire range of 4000-500 cm^{-1} (a) and in the smaller range of 2000-1000 cm^{-1} (b)) tested at pH 9. The arrows indicate the formation of the catechol-boronate complex at 1495 cm^{-1}.

Table S3. Statistical analysis for W_{adh} and S_{adh} of adhesive hydrogel-coated structures of different ARs while varying the preload from 10-80 mN at pH 3 (n = 3). W_{adh} and S_{adh} for compositions at a particular preload not connected by the same letter are significantly different.

	W_{adh}				S_{adh}			
Composition	10	20	40	80	10	20	40	80
AD-AR0.4	A	A	A	A	A	A	A	A
AD-AR1	B	B	B	B	A	A	B	B
AD-AR2	C	C	C	C	B	B	C	C

Table S4. Statistical analysis for W_{adh} (a) and S_{adh} (b) of adhesive hydrogel-coated structures of different ARs while varying the preload from 10-80 mN at pH 3 (n = 3). W_{adh} or S_{adh} at preload values for a given composition not connected by the same letter are significantly different.

	AD-AR0.4		**AD-AR1**		**AD-AR2**	
Preload	**W_{adh}**	**S_{adh}**	**W_{adh}**	**S_{adh}**	**W_{adh}**	**S_{adh}**
10	A	A	A	A	A	A
20	A	A	A	A	A	A
40	B	A B	B	A	A	A B
80	B	B	B	A	A	B

Table S5. Statistical analysis for W_{adh} and S_{adh} of adhesive hydrogel-coated structures of different ARs while varying the preload from 10-80 mN at pH 9 (n = 3). W_{adh} and S_{adh} for compositions at a particular preload not connected by the same letter are significantly different.

	W_{adh}				**S_{adh}**			
Composition	10	20	40	80	10	20	40	80
AD-AR0.4	A	A	A	A	A	A	A	A
AD-AR1	A	A	A	A	A	A	A	A
AD-AR2	A	A	A	A	A	A	A	A

Table S6. Statistical analysis for W_{adh} and S_{adh} of adhesive hydrogel-coated structures of different ARs while varying the preload from 10-80 mN at pH 9 (n = 3). W_{adh} or S_{adh} at preload values for a given composition not connected by the same letter are significantly different.

	AD-AR0.4		**AD-AR1**		**AD-AR2**	
Preload	**W_{adh}**	**S_{adh}**	**W_{adh}**	**S_{adh}**	**W_{adh}**	**S_{adh}**
10	A	A	A	A	A B	A
20	A	A	A	A	A	A
40	A	A	A	A	B	A
80	A	A	A	A	C	A

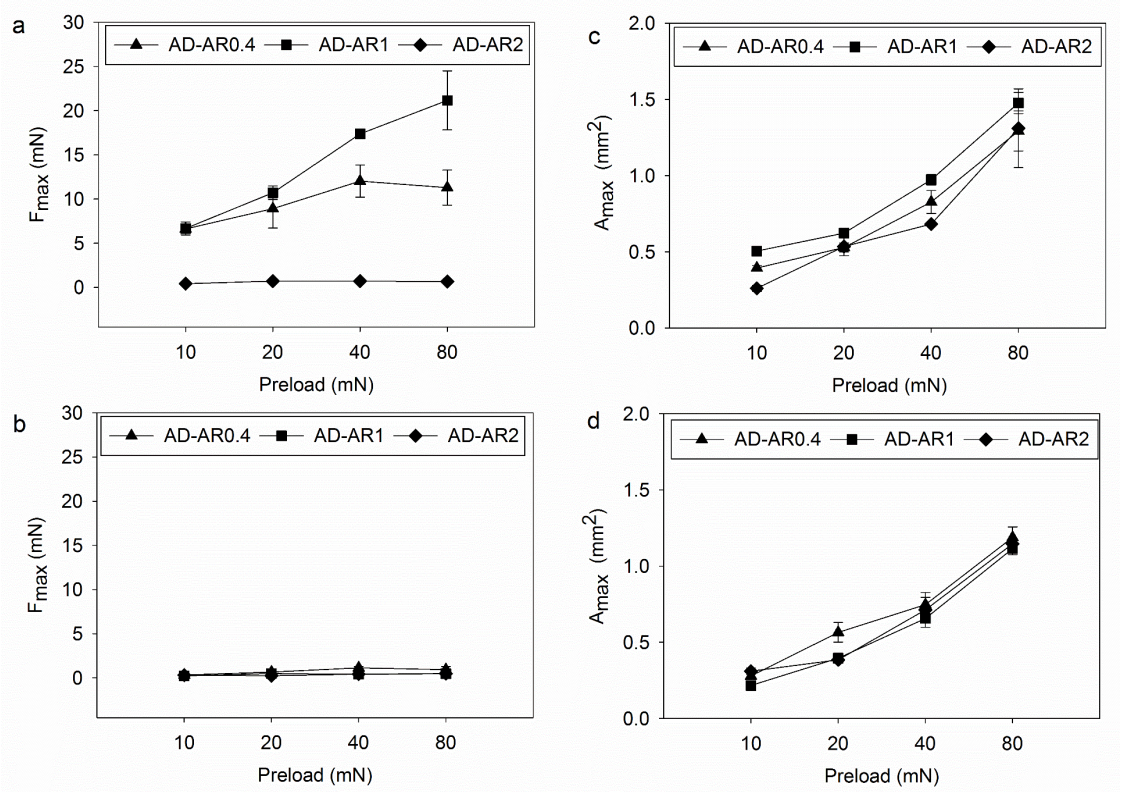

Figure S5. F_{max} (a, b) and A_{max} (c, d) of adhesive hydrogel-coated micropillars tested with varying preload at pH 3 (a, c) and 9 (b, d) (n = 3). Refer to Tables S7-S10 for statistical analysis.

Table S7. Statistical analysis for F_{max} and A_{max} of adhesive hydrogel-coated structures of different ARs while varying the preload from 10-80 mN at pH 3 (n = 3). F_{max} or A_{max} at preload values for a given composition not connected by the same letter are significantly different.

	AD-AR0.4		**AD-AR1**		**AD-AR2**	
Preload	**F_{max}**	**A_{max}**	**F_{max}**	**A_{max}**	**F_{max}**	**A_{max}**
10	A	A	A	A	A	A
20	A	A	A	A	A	A
40	A	B	B	B	A	A
80	A	C	B	C	A	B

Table S8. Statistical analysis for F_{max} and A_{max} of adhesive hydrogel-coated structures of different ARs while varying the preload from 10-80 mN at pH 3 (n = 3). F_{max} or A_{max} for compositions at a particular preload not connected by the same letter are significantly different.

	F_{max}				**A_{max}**			
Composition	10	20	40	80	10	20	40	80
AD-AR0.4	A	A	A	A	A	A	A B	A
AD-AR1	A	A	B	B	B	A	A	A
AD-AR2	B	B	C	C	C	A	B	A

Table S9. Statistical analysis for F_{max} and A_{max} of adhesive hydrogel-coated structures of different ARs while varying the preload from 10-80 mN at pH 9 (n = 3). F_{max} or A_{max} at preload values for a given composition not connected by the same letter are significantly different.

	AD-AR0.4		**AD-AR1**		**AD-AR2**	
Preload	**F_{max}**	**A_{max}**	**F_{max}**	**A_{max}**	**F_{max}**	**A_{max}**
10	A	A	A	A	A	A
20	A B	B	A	B	A	A
40	B	C	A	C	A	B
80	A B	D	A	D	A	C

Table S10. Statistical analysis for F_{max} and A_{max} of adhesive hydrogel-coated structures of different ARs while varying the preload from 10-80 mN at pH 9 (n = 3). F_{max} and A_{max} for compositions at a particular preload not connected by the same letter are significantly different.

	F_{max}				**A_{max}**			
Composition	10	20	40	80	10	20	40	80
AD-AR0.4	A	A	A	A	A	A	A	A
AD-AR1	A	A	B	A	B	B	A	A
AD-AR2	A	A	B	A	A	B	A	A

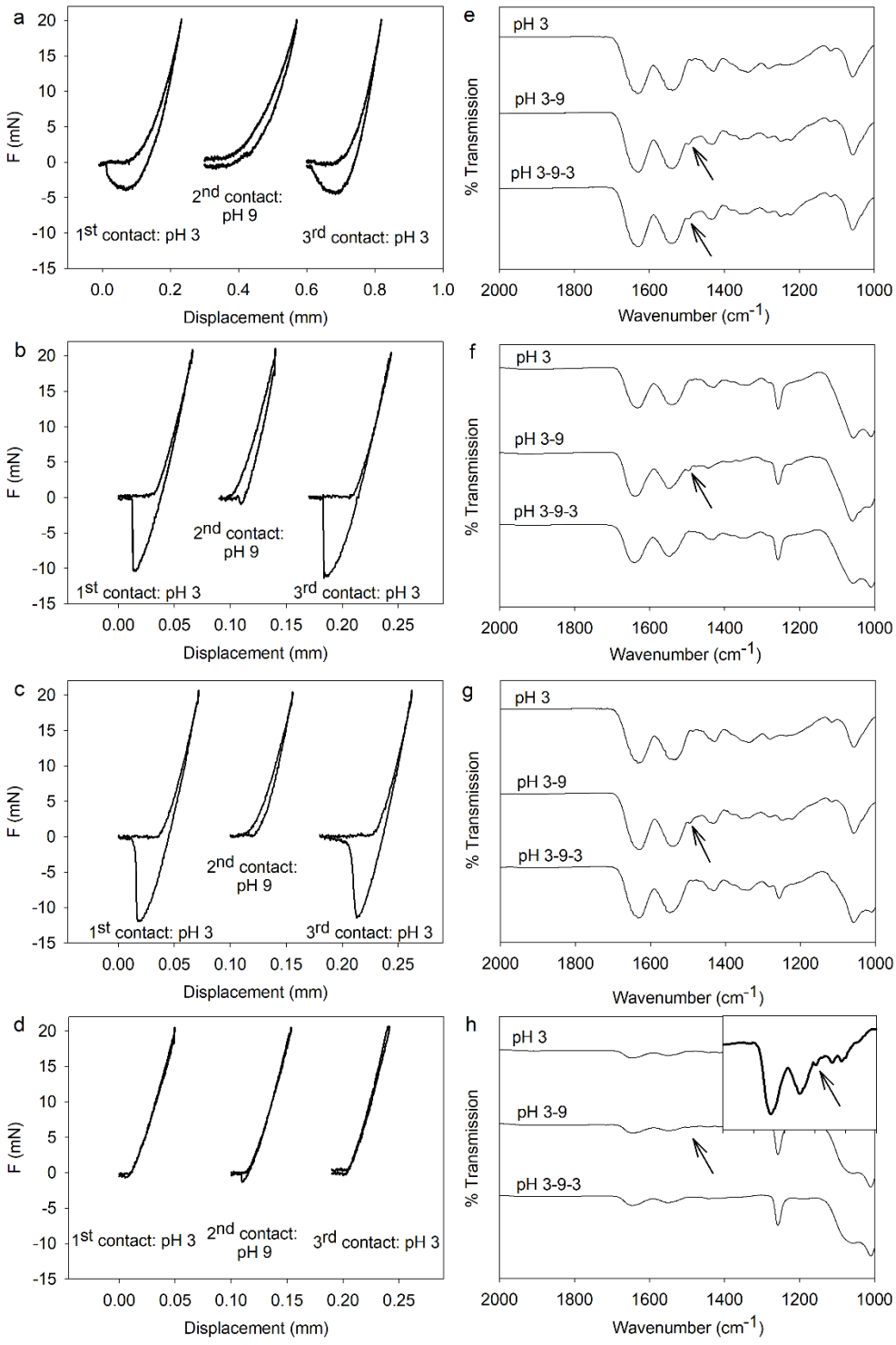

Figure S6. Three successive contact curves of the compositions (left column, a-d) and their corresponding FTIR spectra (right column, e-h) for AD-Flat (a-e), AD-AR0.4 (b-f), AD-AR1 (c-g), and AD-AR2 (d-h) tested at pH 3, pH 9 and then pH 3 using a SiO_2 hemisphere. The arrows indicate the formation of the catechol-boronate complex at 1495 cm^{-1}. The inset image in (h) shows the presence of the complex at a zoomed in scale.

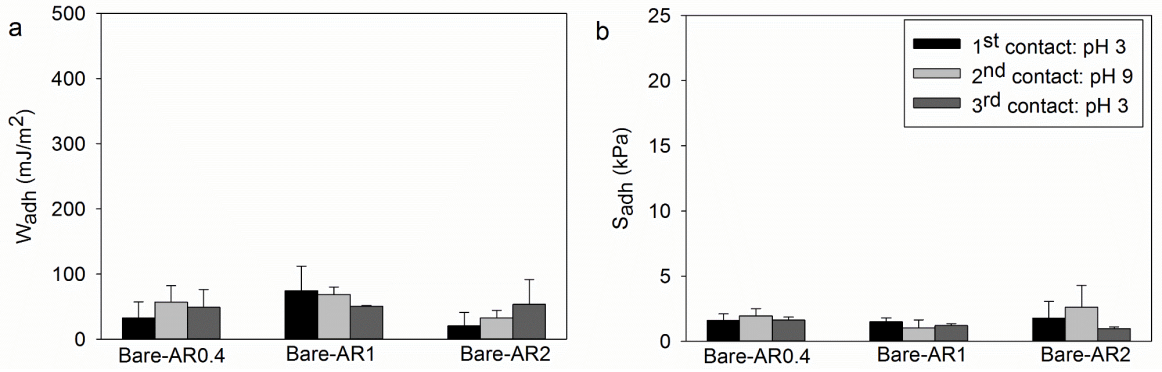

Figure S7. Work of adhesion (W_{adh}) (a) and strength of adhesion (S_{adh}) (b) of bare templates of different ARs tested in 3 successive contact cycles using a SiO_2 hemisphere (n = 3). Refer to Tables S12-S15 for further statistical analyses.

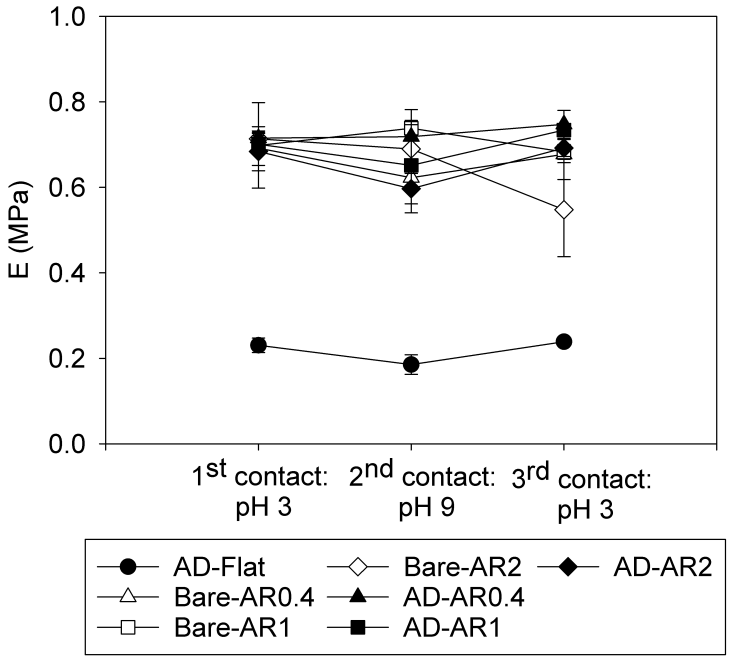

Figure S8. Young's modulus (E) of AD-Flat, bare templates and adhesive hydrogel-coated structures of different ARs tested in 3 successive contact cycles (n = 3). Refer to Table S11 for statistical analysis.

Table S11. Statistical analysis for the Young's modulus (E) of AD-Flat, bare templates and adhesive hydrogel-coated structures of different ARs tested in 3 successive contact cycles using a SiO_2 hemisphere (n = 3). E at contact cycle values for a given composition not connected by the same letter are significantly different.

E							
Cycle #	**Bare-AR0.4**	**Bare-AR1**	**Bare-AR2**	**AD-Flat**	**AD-AR0.4**	**AD-AR1**	**AD-AR2**
1st contact: pH 3	A	A	A	A B	A	A	A
2nd contact: pH 9	A	A	A	B	A	A	A
3rd contact: pH 3	A	A	A	A	A	A	A

Table S12. Statistical analysis for the work of adhesion (W_{adh}) of AD-Flat, bare templates and adhesive hydrogel-coated structures of different ARs tested in 3 successive contact cycles using a SiO_2 hemisphere (n = 3). W_{adh} at contact cycle values for a given composition not connected by the same letter are significantly different.

W_{adh}							
Cycle #	**Bare-AR0.4**	**Bare-AR1**	**Bare-AR2**	**AD-Flat**	**AD-AR0.4**	**AD-AR1**	**AD-AR2**
1st contact: pH 3	A	A	A	A	A	A	A
2nd contact: pH 9	A	A	A	A	A	B	A
3rd contact: pH 3	A	A	A	A	A	A	A

Table S13. Statistical analysis for W_{adh} of AD-Flat, bare templates and adhesive hydrogel-coated structures of different ARs tested in 3 successive contact cycles using a SiO_2 hemisphere (n = 3). W_{adh} of compositions during a particular contact cycle not connected by the same letter are significantly different.

	W_{adh}		
Composition	**1st contact: pH 3**	**2nd contact: pH 9**	**3rd contact: pH 3**
Bare-AR0.4	A	A	A
Bare-AR1	A	A	A
Bare-AR2	A	A	A
AD-Flat	B	A	B
AD-AR0.4	B	A	B C
AD-AR1	C	A	C
AD-AR2	A	A	A

Table S14. Statistical analysis for the strength of adhesion (S_{adh}) of AD-Flat, bare templates and adhesive hydrogel-coated structures of different ARs tested in 3 successive contact cycles using a SiO_2 hemisphere (n = 3). S_{adh} at contact cycle values for a given composition not connected by the same letter are significantly different.

S_{adh}							
Cycle #	**Bare-AR0.4**	**Bare-AR1**	**Bare-AR2**	**AD-Flat**	**AD-AR0.4**	**AD-AR1**	**AD-AR2**
1st contact: pH 3	A	A	A	A	A	A	A
2nd contact: pH 9	A	A	A	B	B	B	A
3rd contact: pH 3	A	A	A	A	A	A	A

Table S15. Statistical analysis for S_{adh} of AD-Flat, bare templates and adhesive hydrogel-coated structures of different ARs tested in 3 successive contact cycles using a SiO_2 hemisphere (n = 3). S_{adh} of compositions during a particular contact cycle not connected by the same letter are significantly different.

	S_{adh}		
Composition	**1st contact: pH 3**	**2nd contact: pH 9**	**3rd contact: pH 3**
Bare-AR0.4	A	A	A
Bare-AR1	A	A	A
Bare-AR2	A	A	A
AD-Flat	A	A	A
AD-AR0.4	B	A	B
AD-AR1	B	A	B
AD-AR2	A	A	A

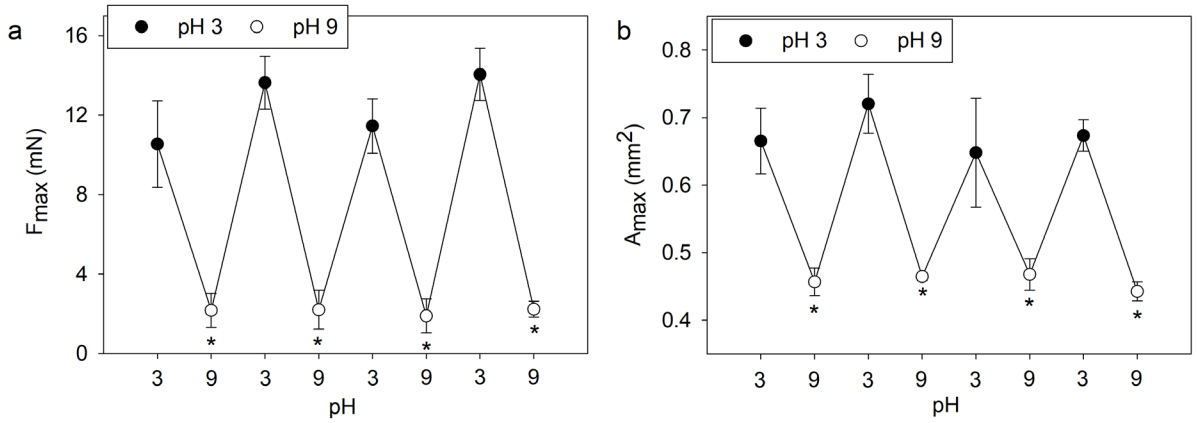

Figure S9. F_{max} (a) and A_{max} (b) of AD-AR1 showing multiple adhesion on/off cycles with alternate incubations at pH 3 and pH 9 (n = 3). $^{*}p < 0.05$ when compared to the preceding pH 3 contact.

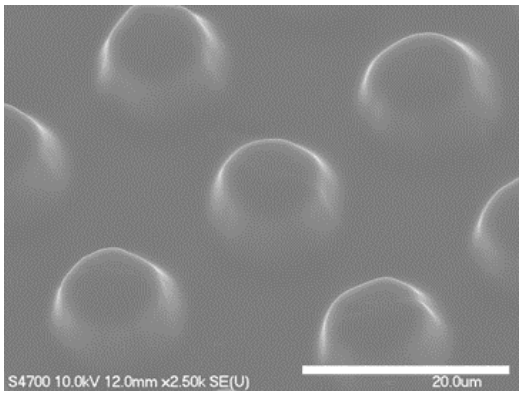

Figure S10. Representative FE-SEM image of AD-AR1 after repeated contact cycles with changing pH. Scale bar = 20 μm.